nature machine intelligence

Article

https://doi.org/10.1038/s42256-023-00764-9

Bridging the gap between chemical reaction pretraining and conditional molecule generation with a unified model

Received: 14 March 2023

Accepted: 25 October 2023

Published online: 05 December 2023

Check for updates

Bo Qiang[1], Yiran Zhou[1], Yuheng Ding[1], Ningfeng Liu[1], Song Song[1], Liangren Zhang[1], Bo Huang[2] ✉ & Zhenming Liu[1] ✉

Chemical reactions are the fundamental building blocks of drug design and organic chemistry research. In recent years, there has been a growing need for a large-scale deep-learning framework that can efficiently capture the basic rules of chemical reactions. In this paper, we have proposed a unified framework that addresses both the reaction-representation learning and molecule generation tasks, which allows for a more holistic approach. Inspired by the organic chemistry mechanism, we develop a new pretraining framework that enables us to incorporate inductive biases into the model. Our framework achieves state-of-the-art results in performance of challenging downstream tasks. By possessing chemical knowledge, our generative framework overcomes the limitations of current molecule generation models that rely on a small number of reaction templates. In extensive experiments, our model generates synthesizable drug-like structures of high quality. Overall, our work presents a noteworthy step toward a large-scale deep-learning framework for a variety of reaction-based applications.

Deep-learning models have found applications across a multitude of scientific research domains[1–3]. Pretraining frameworks[4,5] facilitate the seamless integration of new tasks, thereby expediting the modelling process, especially for scenarios with limited labelled data.

Chemical reactions are the foundation of drug design and organic chemistry studies. Currently, data-mining research and application[6,7] have enabled deep-learning models to be applied to chemical reactions. Based on these data, there has been much data-driven research that delves into the representation learning of chemical reactions. Representation learning refers to automatically learning useful features from the data, which can then be used for various downstream tasks[8]. In earlier works, traditional molecular fingerprints were applied directly for reaction representations[9,10]. Inspired by natural language processing methods, researchers also applied attention-based network[11,12] or contrastive learning techniques[13,14] in chemical reaction pretraining networks. These representations have been tested on classification tasks[15] or regression tasks[16]. However, these methods ignore the fundamental theories in organic chemistry, limiting their performance. For example, electronic effects and inductive effects will be ignored if bonds or atoms outside the reactive centres are masked[13].

Aside from reaction classification tasks, molecule generation based on chemical reactions is also an important application. This branch of modelling has been proven generate synthetically accessible molecules[17–20]. Earlier work always applied a step-wise template-based molecule generation strategy.

These template-based methods depend heavily on predefined building blocks and reactions, which narrow down the accessible chemical space. Similar trends are found in the field of reaction product prediction, in which template-based methods[21] cannot be extrapolated to complex reactions; this problem is solved by using template-free methods[22,23]. In the reaction-based molecule generation task, template-free

[1]State Key Laboratory of Natural and Biomimetic Drugs, School of Pharmaceutical Sciences, Peking University, Beijing, China. [2]Beijing StoneWise Technology Co., Ltd, Beijing, China. ✉e-mail: huangbo@stonewise.cn; zmliu@bjmu.edu.cn

https://doi.org/10.1038/s42256-023-00764-9

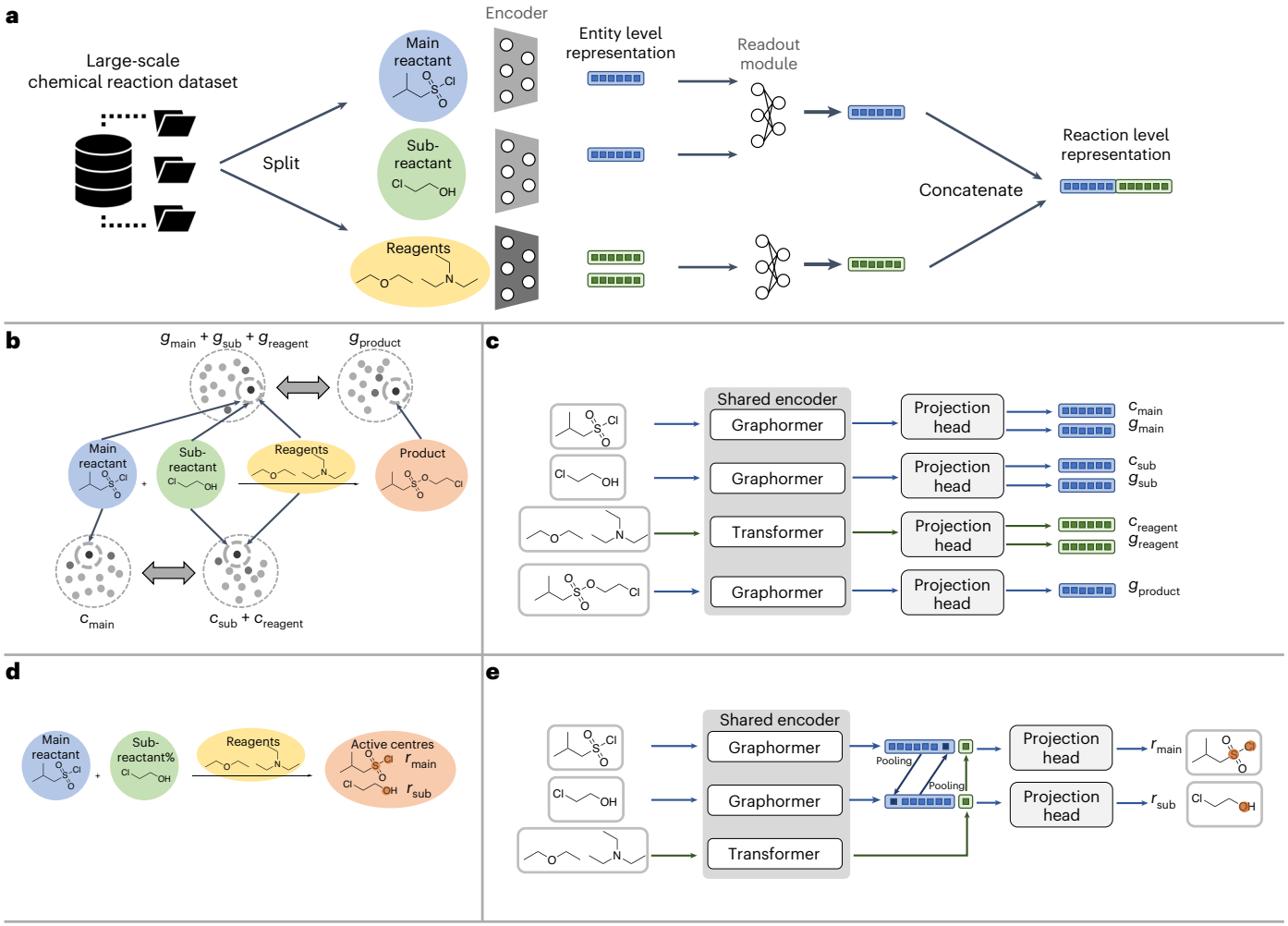

Fig. 1 | Components and methods of Uni-RXN. a, An overview of the unified framework of Uni-RXN. After being split and encoded, entity-level representations are fused into reaction-level representations. **b**, Two contrastive learning tasks we utilized for pretraining. The similarity is maximized between the embeddings of main reactant and {subreactants, reagents}, as well as of {main reactant, subreactants, reagents} and product. **c**, The model architecture for contrastive learning. **d**, An illustration of the reactive centre prediction task. **e**, The model architecture for reactive centre prediction tasks. Projection heads are applied to identify the place where chemical bonds are broken or newly formed in chemical reactions.

methods[24,25] have also demonstrated advantages in generalization over template-based methods. However, existing template-free molecule generation methods can only generate molecules based on predefined reactant libraries. In addition to that, it is more favourable to utilize chemical reactions as editing tools to modify the given structure, regarding the hit-to-lead or lead-optimization phase in drug design. The generated chemical library will focus on a subset of chemical space that could be synthesized with fewer reaction steps.

In this paper, we present a new and comprehensive deep-learning framework for chemical reactions. Our framework, which we call Uni-RXN, is designed to address two fundamental tasks: self-supervised representation learning and conditional generative modelling. Unlike existing approaches, we propose a set of meticulously crafted self-supervised tasks specifically tailored for chemical reactions. These tasks include reactive centre prediction, main reactant to subreactant pairing and reactant–product pairing. In extensive evaluations of challenging reaction tasks, our method surpasses the state-of-the-art, demonstrating its ability to effectively capture domain knowledge of chemical reactions. The promising results obtained pave the way for a wide range of downstream applications.

By efficiently capturing chemical rules, our model is well suited for generative tasks. Unlike conventional approaches that rely on selecting fragments from predefined reactant libraries, our model takes molecular structures as input conditions and produces representations of corresponding reactants while preserving permutation invariance within reactions. Leveraging the power of a dense vector similarity search package, our model enables efficient retrieval of reactants from a large reactant and reagent library. Subsequently, a reaction prediction model is employed to generate product outputs. In comparison to template-based methods that explore only a limited subset of the chemical space, our approach demonstrates superior performance in generating a broader range of synthetically accessible drug-like structures. This characteristic makes our method particularly suitable for virtual library enumeration, as supported by comprehensive statistical analyses and by the case study.

Results and discussion

Challenges in chemical reaction modelling

There are several ways to convert chemical reactions into machine-readable structural data. We define the chemical reactions in the following form:

$$\{Reactant_i\}, i \in m \xrightarrow{\{Reagent_j\}, j \in n} \text{Product} \quad (1)$$

Table 1 | The accuracy of the chemical reaction classification

Reaction number per Class	Rxnrep	MolR	DRFP	Uni-RXN
4	0.169±0.0227	0.249±0.0165	0.258±0.0382	**0.587±0.0229**
8	0.225±0.0080	0.328±0.0173	0.343±0.0159	**0.680±0.0256**
16	0.305±0.0106	0.429±0.0213	0.424±0.0108	**0.754±0.0170**
32	0.375±0.0159	0.526±0.0076	0.498±0.0059	**0.806±0.0101**
64	0.439±0.0078	0.615±0.0022	0.559±0.0044	**0.841±0.0050**
128	0.489±0.0036	0.692±0.0025	0.617±0.0059	**0.865±0.0030**

The accuracy is computed multiple times on different random samples. The data are presented as mean±standard deviation. The higher accuracy indicates better performance. Trained graph neural network encoders from Rxnrep[13] and MolR[14] are applied to compute the baseline model representation. The package that computes the DRFP[10] representation is downloaded directly from the official repository[44]. Bold numbers indicate the best performances.

Chemical reactions involve three main components: reactants, reagents and product. Reactants are structures that contribute certain substructures to form the products, and the reactant whose atoms are maximally matched with the product is defined as the main reactant. Other reactants are denoted as subreactants. Reagents are chemical entities that do not map to any atoms in the product structures but are necessary for providing a certain chemical environment, such as solvents or acids. To jointly model the probability of reactants, reagents and products, there are three primary challenges.

First, complicated organic chemical mechanisms are hard to model. However, we can sum up these mechanisms with a simpler proposition: If we change the subreactants or reagents in an optimized chemical reaction, there is a high likelihood that the reaction will no longer be optimized. This proposition summarized underlying rules within reaction data and enabled us to pretrain our model using the contrastive objective.

Second, it is imperative for the reactants and reagents to exhibit permutation invariance during the modelling process; however, a significant number of models have disregarded this essential aspect. The final challenge is that reactants and reagents play different roles in chemical reactions, which makes the modelling challenging.

To address these challenges, we design a new unified framework for modelling chemical reactions. The first challenge that results from the reaction's complicated underlying mechanism is solved by contrastive learning and by the reactive centre prediction task, which is discussed in the section 'Self-supervised contrastive learning'. The second equivariant challenge is solved by shared parameters in encoding, as in Fig. 1a and a permutation invariant generative network in the generative process. The last challenge is solved by applying a multimodal network for reactants and reagents, which extract information in different ways. Specifically, a graph-based transformer—that we denoted as 'graphormer' in the figures—is applied to process reactants and products, and a text-based transformer is applied to process reagents. We discuss the pretraining and the generative models respectively in sections 'Self-supervised contrastive learning' and 'Conditional generation framework'.

Pretraining framework and downstream tasks

Self-supervised contrastive learning. The key components of contrastive learning are the methods of negative data sampling. Rather than dropping or masking atoms outside the reactive centre, which would result in a loss of information, we adopt a different strategy, as illustrated in Fig. 1b,d. Our model tends to encode two fundamental aspects of chemical reactions.

First, we model the interactivity between the main reactant and the combination of subreactant and reagents (denoted as {subreactants, reagents} for emphasis below). It is well recognized that the dataset of the chemical reactions is biased. Specifically, only optimized and widely used chemical reactions are curated in the public patent datasets. Therefore, the model trained only on the public dataset will fail to capture any information of negative data (that is, invalid reactions). To address this, we apply contrastive loss on reactants and reagents, where the negative samples are generated by the random permutation of subreactants and reagents among the positive reactions (Methods). We use information noise-contrastive estimation (infoNCE) as the training objective, projecting the embeddings of the main reactant and {subreactants, reagents} into the same embedding space with different multi-layer perception (MLP) projection models. When there are multiple subreactants or reagents, a readout module is applied. This approach maximizes the similarity between paired main reactants and {subreactants, reagents} in the embedding space. The training objective is inspired by the powerful generative pretraining model GPT-2/3 (ref. 26) where the main reactant and {subreactants, reagents} in our model mimic its context and next time-step token, respectively, enabling us to develop the conditional generative model that is discussed in detail in the section 'Conditional generation framework'.

Second, we seek to model the functional group rearrangement and structure transformation between the combination of main reactant, subreactants and reagents (denoted as {main reactant, subreactants, reagents} for emphasis) and product. Under the chemical condition provided by the reagents, the functional group within the main reactant and subreactants are rearranged. To learn this transformation process, based on the same encoder, we apply another set of projection heads to predict the embeddings of {main reactant, subreactants, reagents} and product. A similar training process is performed as the first contrastive learning task, in which the paired similarity between {main reactant, subreactants, reagents} and product in the embedding space is maximized. The model architecture is depicted in Fig. 1c.

By leveraging these two fundamental aspects of chemical reactions, our contrastive learning framework is able to learn from biased and unoptimized data and generate rich representations.

Reactive centre prediction. Aside from contrastive learning, our model is also trained to predict the reactive centres in chemical reactions, as in Fig. 1e. In our work, we define atoms as chemical reactive centres if they undergo chemical state change. The chemical state is defined as the formal charge, the hybridization and the neighbour atom types of a certain atom. We propose to use another graph-based transformer (graphormer) model instead of MLP as the projection head, which will be discussed in detail in Methods. This pretraining task further helps our model to understand the position effect in chemical reactions, which has been ignored in related research.

Reaction classification. After completing the two pretraining tasks on the USTPO MIT dataset[22], we use the shared encoder to generate representations for downstream tasks. To ensure a fair comparison, we do not split the main reactants and subreactants when generating representations.

The results of reaction classification on the TPL 1k dataset[11] are provided in the Supplementary Information. In addition, we evaluate

https://doi.org/10.1038/s42256-023-00764-9

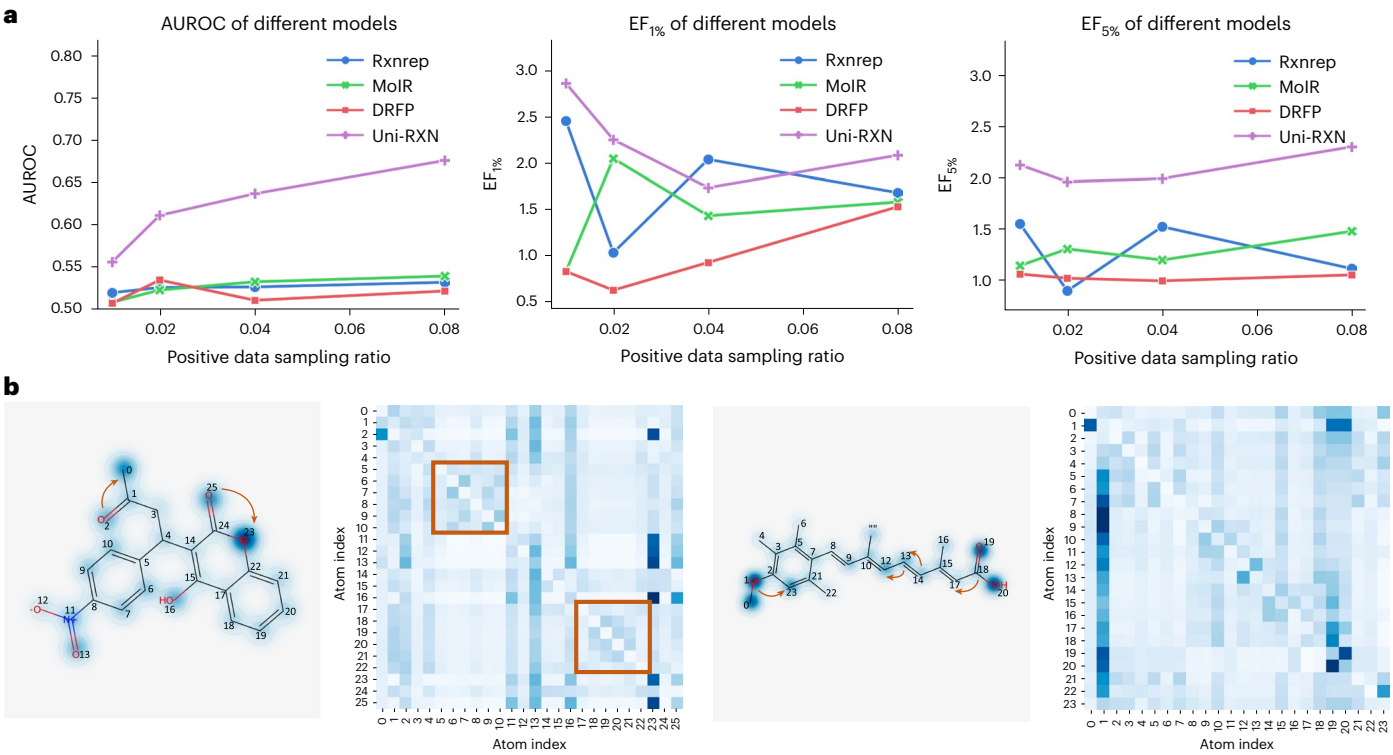

Fig. 2 | Retrieval performance and attention weights of Uni-RXN. a, The line charts illustrate the AUROC, $EF_{1\%}$ and $EF_{5\%}$ of different representations in the chemical reaction retrieval task. **b**, The attention map of the graph-based transformer encoder. Atoms that belong to the same functional group have high cross-attention which demonstrates that our model is capable of learning position effect and identifying reactive atoms.

Uni-RXN on the more challenging Schneider[9] classification dataset, which used a comprehensive ontology system to classify reactions into superclass and secondary classes. We have removed the reactions with templates found in our test set from the pretraining stage.

When generating the representation, we mask the product of the chemical reactions to prevent the model from relying on simple graph pattern recognition. To make the classification even harder, we balanced the dataset by randomly drawing the same number of reactions for each class both in the training and testing dataset, following previous work[13]. Three other available methods are also used to provide for a comparison regarding the accuracy of our method. The results on this balanced benchmark dataset are presented in Table 1.

Logistic regression classification is applied here as the reaction classification heads based on the chemical reaction representations. We compared Uni-RXN with three baseline models. The accuracy of predicting the correct reaction class drastically decreases when the number of reactions per class drops from 128 to 4. In the range of dataset sizes we tested, our model has outperformed the baseline models by a large margin, especially on small training sets. Our model predicts more than half of the reaction classes with only four reactions per class for training. Notably, we keep the encoder parameter fixed when comparing our model with other baselines. Our model demonstrates impressive results without fine-tuning any pretrained parameters. In conclusion, Uni-RXN is a powerful tool to classify chemical reactions even without product information, showing great potential in reaction forward prediction applications.

Reaction retrieval. We evaluate our model's ability to distinguish optimized reactions from unoptimized reactions using the reaction retrieval task. This evaluation ensures the effective implementation of our chemical informative representation in the generative model, preventing the generation of suboptimal reactions. We curated a dataset, as described in Methods, comprising positive examples of successful reactions and negative examples of noisy or suboptimal reactions. This dataset serves as a reliable benchmark for assessing our model's capability to identify optimized reactions.

We conduct experiments using different positive data sampling ratios ranging from 0.01 to 0.08, chosen to simulate real-world scenarios where only a relatively small proportion of reactions are optimized. As depicted in Fig. 2a, our model outperforms other baseline models in most settings. The enrichment factor (EF) results prove that even if less than 1% of data are positive results, Uni-RXN is capable of differentiating the optimized reactions from unoptimized ones. We also provide results on a different template-based negative reaction sampling method[27] in the Supplementary Information, where Uni-RXN also outperforms the baseline models. In conclusion, our representation can be applied to reaction retrieval tasks, even with extremely limited positive data, and holds the potential to assist chemists in identifying the correct reagents and subreactants for high-yield organic reactions.

Visualization of attention. The visualization of the Transformer attention sheds light on the model's processing of the input graph, providing insights into its performance on the above two important downstream tasks. To examine this, we present the attention weights in Fig. 2b. The attention maps clearly illustrate that our model learns to focus on the reactive portion of the input main reactant molecules. Notably, heteroatoms in active groups such as ester group which play crucial roles in chemical reactions, exhibit higher attention scores compared to carbon chains and other heteroatoms. Moreover, our model captures more intricate rules involving interactions between neighbouring functional groups. For instance, when a benzene ring possesses a strong electron-withdrawing group, the ortho-position becomes more reactive, and our encoder effectively captures this fundamental chemical rule by directing attention to the ortho-position. Furthermore, the

https://doi.org/10.1038/s42256-023-00764-9

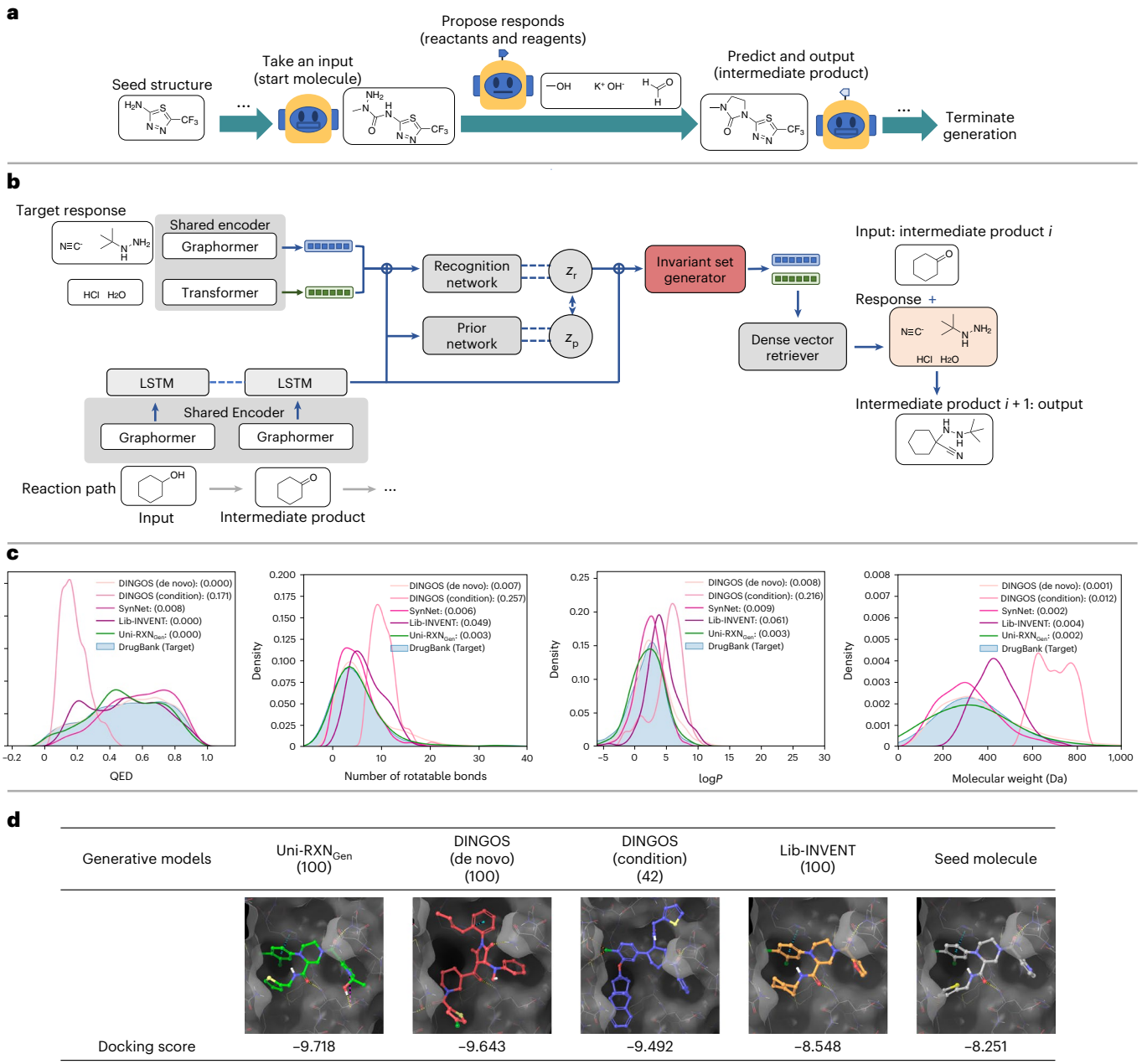

Fig. 3 | Process and performance of Uni-RXN$_{Gen}$. a, An overview of the generation framework. A sequential process is proposed to generate the analogues. At each step, the model proposes the subreactants and reagents; then the reaction predictor outputs the product. The product is fed to the model as the input for the next step until the termination criterion is met. **b**, The model architecture of the generative model. The pretrained model is utilized here as the encoder for target structures and main reactant inputs. **c**, The properties of the drug-like molecule generated by different reaction-based molecular generation models. The molecular mean distance distribution distances are listed within the parentheses. See text for axis descriptions. **d**, The docking pose of the top-scoring generated COVID-19 3CLPro inhibitors. The grey poses are the reference poses of the seed molecule derived from the original Protein Data Bank file. The scaffold of the Uni-RXN$_{Gen}$-sampled molecule and Lib-INVENT-generated molecule aligned perfectly with the reference pose and the Uni-RXN$_{Gen}$-sampled molecule has a higher absolute docking score.

attention maps exhibit well-clustered patterns, with self-attentions between atoms within the same aromatic ring due to their shared electron cloud. Conversely, the attention between neighbouring functional groups receives higher scores, as their relationships define the behaviour of reactants in organic chemical reactions.

Conditional generation framework

Our model not only excels in classification tasks but also offers a valuable tool for studying the structure–activity relationship (SAR) in medicinal chemistry research. By leveraging the power of our pretrained encoder, we enable the generation of multiple synthesizable analogues from a given hit structure. This streamlined approach provides researchers with a simplified method for exploring SAR and designing focused chemical libraries. However, generating analogues through chemical reactions on a seed structure poses a challenge.

Template-based methods simplify conditional molecule generation by confining sampling in an infinite space to a predefined subspace, reducing the size of the search area. However, limitations arise when the available subspace becomes limited or empty, restricting direct template application.

https://doi.org/10.1038/s42256-023-00764-9

Table 2 | Evaluation of synthetic accessibility scores, validity, chemical distance and scaffold diversity

	SAScore ↓	RA ↑	Valid (%)	Chemical distance	Mol diversity	Scaffold entropy
Seed molecules	3.631	0.703	–	–	0.906	6.23
SynNet	2.941	0.847	66.61	0.450	0.897	5.77
DINGOS (de novo)	3.080	0.788	100.00	0.602	0.899	5.53
DINGOS (condition)	3.845	0.636	45.81	0.824	0.424	5.60
Lib-INVENT (condition)	3.710	0.558	100.00	0.681	0.869	5.37
Uni-RXN	3.643	0.725	100.00	0.362	0.925	6.09

The down arrow indicates that the lower score means the molecules are easier to synthesize, while the up arrow indicates that the higher score means the molecules are easier to synthesize. 'Valid' indicates the proportion of drug structures for which the model is capable of generating valid analogues. 'Chemical distance' measures the ECFP4 distance between the generated molecule and the input. 'Mol diversity' and 'scaffold entropy' measure the diversity on the full structure level and scaffold level.

Table 3 | The similarity between seed molecules and generated molecules, and the docking scores and diversity of the generated analogues

	DINGOS(de novo)(100)	DINGOS(condition)(42)	Lib-INVENT(100)	Uni-RXN$_{Gen}$(100)
Similarity$_{mean}$	0.2977	0.6548	0.6942	0.7748
Similarity$_{top}$	0.3816	0.7155	0.8163	0.8854
Diversity	0.7913	0.3184	0.3455	0.3949
Docking Score$_{mean}$	−6.5068	−7.7953	−7.5420	−7.8301

The number of the generated molecules we docked with the protein pocket is listed in the parentheses in each column header. We kept the 100 analogues that have the closest Jaccard distance to the input molecules for docking. However, the DINGOS (condition) model is only able to generate 42 valid molecules.

To overcome these challenges, we develop a template-free generative model that efficiently generates chemical reaction paths. Each path consists of a series of reactions where the product of the previous reaction is the main reactant of the subsequent reaction. Such paths simulate human experts who utilize chemical reactions to expand the chemical space based on the seed molecule. A conditional variational encoder network, denoted as Uni-RXN$_{Gen}$ is trained to generate reaction paths autoregressively by approximating the likelihood of subreactants and reagents based on the reaction path from previous steps, as illustrated in Fig. 3a.

The architecture of our model is depicted in Fig. 3b. Instead of generating the subreactants and reagents directly, we generate the representations of these molecules' structures. Two separate encoders extract the information from the reaction path condition and the target responses. Then the invariant generator decodes the latent variable to generate the target representations. After Uni-RXN$_{Gen}$ generates the target representations, a dense vector retriever is used to search for reactants and reagents in a large commercially accessible molecule library. Based on the input main reactant and the retrieved subreactants and reagents, another network predicts the product of the proposed new reactions. In short, Our model provides an efficient and effective workflow for generating chemical analogues by sampling reactions and predicting the results sequentially.

To evaluate our model's capacity of generating similar molecule structures conditioned on the input seed molecules, we use 2,567 structures from the Drugbank database[28] to derive large drug-like datasets using our generative model. We compared our model with four baseline models, SynNet[19], Lib-INVENT[29], DINGOS (de novo) and DINGOS (condition)[18].

Properties evaluation. To evaluate the quality of the generated structures, we computed several basic drug-like properties and compared them with real drugs, as illustrated in Fig. 3c. Our goal is to generate molecules that closely resemble real drugs in terms of their property data distribution. It is evident that DINGOS (condition) generates molecules with a shifted chemical property distribution despite performing only a few steps of reaction modification on the seed molecules. Regarding the metrics of molecular weight and QED, Uni-RXN$_{Gen}$, SynNet and DINGOS (de novo) provide comparable results. However, the baseline methods generate molecules with more lipophilic structures and an increased number of rotatable bonds, unlike our model.

This paper goes beyond assessing the drug-likeness of molecules generated by Uni-RXN$_{Gen}$, as we also use synthetic accessibility scores to evaluate their synthesizability. To accomplish this, we apply two different metrics (SAScore[30] and RA[31]); the results are presented in Table 2.

Three of the methods—our model, DINGOS (condition) and Lib-INVENT—can generate molecules directly from the input structures; the other methods need more reaction steps to generate from scratch. Unlike DINGOS (condition), which generates larger molecules due to the lack of decomposition reaction in the predefined templates, our generated molecules scored favourably on the SAScore and RA metrics, indicating that they are easier to synthesize. Template-based de novo methods, including SynNet and DINGOS (de novo), generate molecules distant from the seed molecules and have obvious distribution shifts on SAScore and RA. These facts and the distance metrics indicate that DINGOS (de novo) and SynNet sacrifice drug similarity and validity for better synthetic accessibility scores, respectively. Thus, the template-based methods tend to generate excessively simple molecules, which is undesirable in drug discovery research. Furthermore, our proposed modifications require fewer reaction steps than a from-scratch, complicated route by multiple template reactions. Overall, our approach provides a more effective way to generate molecules based on available drugs, where (1) fewer chemical reaction steps are required and (2) the generated molecules exhibit a favourable balance between drug similarity and synthetic accessibility.

Validity is an important metric in assessing the performance of a model. SynNet and DINGOS (condition) demonstrate limitations in generating analogues for a limited proportion of input molecules, even though they can generate synthesizable molecules. In addition to validity, we further evaluate molecule diversity and scaffold entropy to assess the models. The results show there are fewer dominant scaffolds and similar molecules within the molecules generated by Uni-RXN$_{Gen}$.

SARS-CoV-2 main protease inhibitor design. Instead of designing new inhibitors[32], we worked to optimize existing ligand structures using our structure-conditional generative model. When generating analogues

of drug-like molecules, maintaining a stable three-dimensional binding conformation is crucial for ensuring that the newly generated molecules can bind to the same protein pockets.

To demonstrate that Uni-RXN$_{Gen}$ generates molecules that fit into the target protein pocket, we conducted a case study on design of an inhibitor for 3CL$_{Pro}$, a coronavirus protease that is a common drug target in current drug research. In our experiment, we generate analogues based on the seed molecule derived from the complex at Protein Data Bank ID 8ACL, with our method, two other reaction-based generative models, namely DINGOS (condition) and DINGOS (de novo)[18,19] and a library design model, Lib-INVENT[29], as shown in Table 3 and Fig. 3d. Our method outperforms other methods on average docking scores and top docking scores when the same number of molecules are kept. Uni-RXN$_{Gen}$ and Lib-INVENT generate top-scored analogues with similar binding conformations and similar topologies, as suggested by the docking results and the fingerprint distances. However, our model still generates molecules of high diversity which outperforms DINGOS (condition) and Lib-INVENT, proving that our model is able to effectively explore the chemical space adjacent to the input seed molecule. We found that the template-based method DINGOS (condition) can only generate 42 valid molecules with the template reactions, proving that reaction templates harm the machine-learning model's ability to explore constrained chemical space. These findings demonstrate that our model can aid medicinal chemists in discovering SAR in a more efficient manner by providing numerous analogues with higher binding affinity.

Conclusion

In this paper, we have presented a new approach to bridge the gap between reaction-based molecule pretraining and generation tasks. Our approach offers several advantages, including the ability to derive rich representations for challenging chemical reaction classification tasks. Uni-RXN outperforms other baseline models by a large margin and achieved 58.7% accuracy with only four data points per class provided. The transformer model can be also applied to differentiate optimized reactions and unoptimized reactions in chemical reaction data. Additionally, the encoder can be effortlessly applied to structure-conditional generation. The experimental results highlight the favourable properties of the molecules generated by our model, making them well suited for drug discovery tasks. Our model is capable of generating molecules with more drug-like properties and synthesizable accessibility. Combined with virtual screening methods, such as molecule docking, this generative model enables efficient SAR studies. The vast synthesizable drug-like chemical space that our model generates can improve the true positive rate in drug repurposing or hit molecule searching.

Methods

Model architecture

Pretraining model. Transformer model. Our pretraining network utilizes two attention-based models as encoders to handle the multimodal nature of chemical reaction data. The reactants and products are encoded by a graph-based transformer model, while the reagents are translated to sequence representation SELFIES[33] and then encoded by a text-based transformer model. The projection heads in contrastive learning tasks are simple MLPs with two layers of hidden parameters to train. We provide a detailed discussion of the two types of transformer models we have designed in the following paragraph.

For the text-based transformer, we base it on the vanilla transformer[34]. However, directly applying the transformer to reagents poses challenges because the tokens within chemical entities follow a sequential order, while the entities themselves are order-agnostic. To address this, we develop a hierarchical transformer to model reagents. In the first step, the sequential tokens are encoded by a vanilla transformer and the embeddings of the classification (CLS) tokens are utilized to represent the entities. Then, a transformer without positional encoding is applied as the readout module for the CLS embeddings of multiple reagents.

The graph-based transformer is inspired by a previous work[35]. Since molecule graphs are permutation invariant, we discarded node positional encoding and applied edge encodings to embed the topological structure of the molecules. The edge feature inputs consist of the bond type and an indicator token that signifies whether the bond belongs to a ring. Similarly, for the node feature, we incorporate the atom element type, the number of formal charges, the hybridization type and a ring indicator. The edge features are applied in our model to get the attention map as follows:

$$A_{ij} = \frac{(h_i W_Q)(h_j W_K)^T}{\sqrt{d}} + b_\phi(e_{ij}) + c_\phi \mathrm{SP}(i,j) \quad (2)$$

where h_i and h_j denote the node embeddings of node i and node j; d is the dimension of the edge features; W_Q and W_K are trainable weight matrices; e_{ij} is the one-hot edge feature (all zeros indicate that there are no edges between them); SP is a function that returns the shortest path from node i to node j; and b_ϕ and c_ϕ are all learnable neural networks. With this modification in attention mechanism, the model is able to capture and encode local structure while maintaining long-range interactions, which are always hard to encode with traditional message-passing neural networks[36]. This function enables our model to learn the interaction between functional groups and understand more complicated organic chemistry. The model can take multiple graphs as input, so we set the shortest path distance between atoms that do not belong to the same reactant molecules as infinity. In this way, the model automatically aggregates information within this hypergraph, where both local and global interactions are enabled.

When this graph-based transformer model is applied, we add an auxiliary node, the virtual node. It is connected to all atoms even if they belong to different molecules. The embeddings of the virtual token can be used as the results of a full graph-level readout. In the reactive centre prediction task, we apply sum pooling to the token level representations from the graph-based transformer and appended the CLS token from the text-based transformer as the additional input to the prediction model, which is illustrated in Fig. 1e. This design maintains permutation invariance and allows efficient information exchange between models.

Training objective. In this section, we discuss the training objective of pretraining. In the first contrastive learning task, we want to model the interaction between reactants. Hence, the InfoNCE Loss is employed to maximize the similarity between the representation of main reactants $x = c_{main}$ and their chemical reaction environment (the subreactants and reagents) $v = c_{sub} + c_{reagent}$, using X to represent all reactants and V to represent all chemical reaction environments.

$$\mathcal{L}_{\mathrm{InfoNCE}} = -\mathbb{E}_X\left[\log \frac{f(x_i, v_i)}{\sum_{x_j \in X} f(x_j, v_i)}\right] - \mathbb{E}_V\left[\log \frac{f(x_i, v_i)}{\sum_{v_j \in V} f(x_i, v_j)}\right]$$

We apply the inner product here as the similarity function f. In the second contrastive learning task, the transformation from reactants to products is modelled by our probabilistic model. The same loss function $\mathcal{L}_{\mathrm{InfoNCE}}$ is applied when $x = g_{main} + g_{sub} + g_{reagent}$ stands for chemical reaction inputs (reactants, reagents) and $v = g_{product}$ stands for chemical reaction outputs (products). To estimate the loss efficiently, the X and V are approximated by in-batch sampled embeddings. For training the reactive centre prediction task, we employ the binary cross entropy loss as our objective function. We apply this to predict multiple reactive centres defined by atoms whose chemical environments have changed.

Generative model. Conditional variational auto-encoder. We build a conditional variational auto-encoder based on the pretrained encoder to generate the representation of the responses (subreactants and reagents). As illustrated in Fig. 3b, we first use a long short-term memory network to collect the embeddings along the reaction paths we sample from the chemical reaction network[37]. Two MLP networks are designed for variational inferencing. The recognition network takes both the target representation and the embeddings of the previous reaction path as inputs, while the prior network processes only the latter. By minimizing the Kullback–Leibler divergence between these dual latent variables, akin to classic variational auto-encoder models, we obtain the latent variable z. Subsequently, the invariant set generator utilizes this latent variable to generate the target representations. During training, the prior network is trained to approximate the distribution generated from the recognition network. During the generation phase, only the latent variable from the prior network is passed forward to the generator.

Invariant set generator. Generating a permutation invariant set presents a challenge, as discussed in previous research[38]. In this study, we propose a similarity-based approach to generate varying numbers of reactant–reagent representations from the latent variable. To accomplish this, we maintain a reference parameter set and employ its angle to determine the selection of data points for representation generation. Let Θ and R denote the angle and latent variable of the reference set with size n_0, respectively. The formulation of the model is as follows:

$$\begin{aligned} a &= \mathrm{MLP}_1(z) \\ c &= \Theta a / \mathrm{vec}((||\theta_i||_2)_{1\le i\le n_0}) \\ s &= \mathrm{argsort}_{\downarrow}(c[:n_{\max}]) \\ \tilde{c} &= \mathrm{softmax}(c[s]) \\ X &= R[s] \odot \tilde{c} W_1 + \tilde{c} W_2 \\ X &= \mathrm{MLP}_2(X, z) \\ Y &= X[i_1, \ldots, i_n], \text{ s.t.} \forall i_x, \mathrm{MLP}_3(X[i_x]) > \delta) \end{aligned} \tag{3}$$

where W_1 and W_2 are trainable weight matrices; MLP_1, MLP_2 and MLP_3 are simple trainable MLP networks; and $n_{\max}$ is the maximum number of responses set in the training set. The threshold δ is applied to decide whether to select the data points. If we use m to represent the dimension of target representations, the output Y will be the $n \times m$ matrix that we need. Instead of using First-N or Top-N set generation methods, we apply a scoring network MLP_3 to determine the size of the set we generate, which helps us to generate more diverse results and update more latent variables during training.

Implementation of forward reaction predictor. We applied the Local-Transformer[39] as our predictor, since it is now the state-of-the-art model for forward reaction prediction. However, any forward reaction prediction model can be plugged into our method without much effort.

Experiment setups

Negative data construction. To construct negative samples, we develop a workflow to sample unsuccessful chemical reactions from the Schneider dataset[9]. Recognizing that different classes of chemical reactions employ distinct subreactants and reagents, we employ various techniques to generate negative samples, namely adding, deleting and switching operations.

In the adding operation, we randomly sample subreactants and reagents from reactions belonging to other reaction classes and append them to the reactions to be perturbed. Conversely, in the deleting operation, random numbers of subreactants and reagents are removed. The switching operation involves replacing random numbers of subreactants and reagents with chemical entities from other reaction classes. Subsequently, we apply a filtering process to refine these perturbed reactions. If the forward reaction product predictor successfully generates the same valid product for our perturbed reactions, they are excluded from the negative sampling dataset. After this filtering, all remaining perturbed reactions are kept and retained as the negative data points.

In addition to our approach, we have also adopted the 'random template' negative sampling strategy from a previous work[27], where reaction templates are applied to select subreactants. The results of this strategy are presented in the Supplementary Information.

Property evaluation. We examine some important drug-like properties and synthetic accessibility scores to prove that our generative model is able to derive drug-like molecules based on drug structures. For DINGOS, Lib-INVENT and Uni-$\mathrm{RXN}_{\mathrm{Gen}}$, multiple structures are generated for the same input. To ensure quantity consistency, we retained the most similar structure within the first eight sampled structures, as measured by ECFP4 Tanimoto similarity.

Molecule weight determines the pharmacokinetics and solubility, which is very important for drug-likeness. The number of rotatable bonds describes the flexibility of three-dimensional molecule conformations, which is important when binding to the target protein. QED[40] is a popular drug-likeness quantized scoring function. Partition coefficient log$P$ is an important physicochemical property when designing drugs. All these property scores are computed by the RDKit package.

SAScore[30] and RA[31] are the synthetic accessibility scores we apply here. SAScore is a rule-based method, in which rare substructures are given a penalty for accessing the synthesizability. The method also accounts for the topological complexity of structures.

RAscore is a scoring function based on neural networks. Numerous synthetic route planning artificial intelligence (AI) models have been developed; however, they are always time consuming when applied to large datasets. RAscore is a classification model trained upon retrosynthetic models. It predicts the probability of a specific structure having a successful route planned by AI agents.

The validity in Table 2 stands for the proportion of seed molecules for which the model is able to generate valid analogues. The maximum depths of tree searching are set to 15, as in the original code repository for SynNet. For DINGOS (condition) model, we regard the generation process as invalid when the input seed molecules do not match with any template reactions for further modifications. In template-free models, the invalid generations represent that the predictor cannot output valid molecule similes or that one reactant is output as the predicted result.

The distance in Table 2 is applied to measure the similarity between generated analogues and input seed molecules. The distance is measured by the mean Jaccard distance on the ECFP4 fingerprint of the analogues and the input seed molecules.

We also use the scaffold diversity to measure the generated molecules. The scaffold diversity is defined as the information entropy as follows:

$$H(\mathrm{S}) = -\sum_{i=1}^{n} P(S_i) \log P(S_i) \tag{4}$$

where $H(\mathrm{S})$ represents the entropy of a random molecule S with scaffold $S_1, S_2, \ldots, S_n$ and $P(S_i)$ is the probability of a molecule having a certain scaffold S_i. Intuitively, a high entropy indicates that the scaffolds are evenly distributed, while a low entropy indicates that there is one or a few dominant scaffolds.

We further evaluate the molecule diversity of the generated molecules from different machine-learning models. The diversity is defined as follows:

$$\mathrm{Div} = \frac{2}{n(n-1)} \sum_{x \neq x' \in \mathcal{G}} 1 - \mathrm{sim}(x, x') \tag{5}$$

where $\mathcal{G}$ is the set of all generated molecules and sim is the ECFP4 Tanimoto similarity function.

Metrics for reaction retrieval. The enrichment factor EF_α is also a widely used metric, which is calculated as

$$EF_\alpha = \frac{NP_\alpha}{NP_t \times \alpha} \quad (6)$$

where NP_α stands for the number of positive samples in the top α predictions and NP_t stands for the number of positive samples in the whole test set. This metric does not rely on the choice of threshold. EF_α is a measurement of the enrichment of positive samples in the top α predictions.

The area under the receiver operating characteristic curve (AUROC) is a widely used metric in binary classification. It quantifies the model's ability to distinguish between positive and negative samples by calculating the area under the ROC curve. The AUROC value ranges from 0 to 1, with higher values indicating better classification performance.

Case study. Using Glide[41], we conduct molecule docking to the $3CL_{Pro}$ protein pocket with all generated or screened molecules. The protein structure is processed by Protein Preparation Wizard. Bond orders and missing side chains are fixed using Prime in the preparation workflow. Waters with less than three H-bonds to amino acids are removed. The docking grid—of size 10 Å × 10 Å × 10 Å in which the centre is defined by the co-crystal ligand—is saved based on the processed protein. The ligands' conformations and possible tautomers and protonation states are generated by the LigPrep module. The ligand conformations are docked into the pocket using Glide[41]. Default settings are applied to other parameters. The Glide docking scores are used to rank the results.

Data availability

The USTPO MIT was downloaded from the official Github repository (https://github.com/wengong-jin/nips17-rexgen) and Schneider datasets were downloaded from the Supplementary Information of the original article[9] (https://pubs.acs.org/doi/suppl/10.1021/ci5006614/suppl_file/ci5006614_si_002.zip). We provide our processed training data in python pickle format at https://doi.org/10.5281/zenodo.8075066 (ref. 42).

Code availability

The code to reproduce the results and Python scripts to reproduce the training data are publicly available at https://github.com/qiangbo1222/Uni-RXN-official (ref. 43).

References

1. Devlin, J., Chang, M.-W., Lee, K. & Toutanova, K. BERT: pre-training of deep bidirectional transformers for language understanding. Preprint at https://doi.org/10.48550/arXiv.1810.04805 (2018).
2. Jumper, J. et al. Highly accurate protein structure prediction with alphafold. *Nature* **596**, 583–589 (2021).
3. Madani, A. et al. Large language models generate functional protein sequences across diverse families. *Nat. Biotechnol.* **41**, 1099–1106 (2023).
4. Hendrycks, D. et al. Pretrained transformers improve out-of-distribution robustness. In *Proc. 58th Annual Meeting of the Association for Computational Linguistics* (eds Jurafsky, D. et al.) 2744–2751 (Association for Computational Linguistics, 2020).
5. Gu, Y. et al. Domain-specific language model pretraining for biomedical natural language processing. *ACM Trans. Comput. Healthc.* **3**, 1–23 (2021).
6. Lowe, D. M. *Extraction of Chemical Structures and Reactions from the Literature*. PhD thesis, Univ. Cambridge (2012).
7. Lowe, D. Chemical reactions from US patents (1976-Sep2016). *figshare* https://doi.org/10.6084/m9.figshare.5104873.v1 (2017).
8. Goodfellow, I., Bengio, Y. & Courville, A. *Deep Learning* (MIT Press, 2016).
9. Schneider, N., Lowe, D. M., Sayle, R. A. & Landrum, G. A. Development of a novel fingerprint for chemical reactions and its application to large-scale reaction classification and similarity. *J. Chem. Inf. Model.* **55**, 39–53 (2015).
10. Probst, D., Schwaller, P. & Reymond, J.-L. Reaction classification and yield prediction using the differential reaction fingerprint DRFP. *Digit. Discov.* **1**, 91–97 (2022).
11. Schwaller, P. et al. Mapping the space of chemical reactions using attention-based neural networks. *Nat. Mach. Intell.* **3**, 144–152 (2021).
12. Irwin, R., Dimitriadis, S., He, J. & Bjerrum, E. J. Chemformer: a pretrained transformer for computational chemistry. *Mach. Learn.* **3**, 015022 (2022).
13. Wen, M., Blau, S. M., Xie, X., Dwaraknath, S. & Persson, K. A. Improving machine learning performance on small chemical reaction data with unsupervised contrastive pretraining. *Chem. Sci.* **13**, 1446–1458 (2022).
14. Wang, H. et al. *International Conference on Learning Representations* (ICLR, 2022).
15. NameRXN (Nextmove Software, 2021); http://www.nextmovesoftware.com/namerxn.html
16. Schwaller, P., Vaucher, A. C., Laino, T. & Reymond, J.-L. Prediction of chemical reaction yields using deep learning. *Mach. Learn.* **2**, 015016 (2021).
17. Korovina, K. et al. ChemBO: Bayesian optimization of small organic molecules with synthesizable recommendations. In *Proc. 23rd International Conference on Artificial Intelligence and Statistics* (eds Chiappa, S. & Calandra, R.) 3393–3403 (PMLR, 2020).
18. Button, A., Merk, D., Hiss, J. A. & Schneider, G. Automated de novo molecular design by hybrid machine intelligence and rule-driven chemical synthesis. *Nat. Mach. Intell.* **1**, 307–315 (2019).
19. Gao, W., Mercado, R. & Coley, C. W. *International Conference on Learning Representations* (ICLR, 2022).
20. Noh, J. et al. Path-aware and structure-preserving generation of synthetically accessible molecules. In *Proc. 39th International Conference on Machine Learning* (eds Chaudhuri, K. et al.) 16952–16968 (PMLR, 2022).
21. Coley, C. W., Barzilay, R., Jaakkola, T. S., Green, W. H. & Jensen, K. F. Prediction of organic reaction outcomes using machine learning. *ACS Cent. Sci.* **3**, 434–443 (2017).
22. Jin, W., Coley, C., Barzilay, R. & Jaakkola, T. Predicting organic reaction outcomes with Weisfeiler–Lehman network. In *Proc. 31st International Conference on Neural Information Processing Systems* (eds Guyon, I. et al.) 2604–2613 (Curran Associates Inc., 2017).
23. Schwaller, P. et al. Molecular transformer: a model for uncertainty-calibrated chemical reaction prediction. *ACS Cent. Sci.* **5**, 1572–1583 (2019).
24. Bradshaw, J., Paige, B., Kusner, M. J., Segler, M. & Hernández-Lobato, J. M. A model to search for synthesizable molecules. In *Proc. 33rd International Conference on Neural Information Processing Systems* (eds Wallach, H. et al.) 7937–7949 (Curran Associates Inc., 2019).
25. Bradshaw, J., Paige, B., Kusner, M. J., Segler, M. & Hernández-Lobato, J. M. Barking up the right tree: an approach to search over molecule synthesis DAGs. *Adv. Neural Inf. Process. Syst.* **33**, 6852–6866 (2020).
26. Radford, A. et al. Language models are unsupervised multitask learners. *OpenAI Blog* **1**, 9 (2019).

27. Genheden, S., Engkvist, O. & Bjerrum, E. J. A quick policy to filter reactions based on feasibility in AI-guided retrosynthetic planning. Preprint at *chemRxiv* https://doi.org/10.26434/chemrxiv.13280495.v1 (2020).
28. Wishart, D. S. et al. Drugbank 5.0: a major update to the drugbank database for 2018. *Nucleic Acids Res.* **46**, 1074–1082 (2018).
29. Fialková, V. et al. LibINVENT: reaction-based generative scaffold decoration for in silico library design. *J. Chem. Inf. Model.* **62**, 2046–2063 (2021).
30. Ertl, P. & Schuffenhauer, A. Estimation of synthetic accessibility score of drug-like molecules based on molecular complexity and fragment contributions. *J. Cheminform.* **1**, 8 (2009).
31. Thakkar, A., Chadimov´a, V., Bjerrum, E. J., Engkvist, O. & Reymond, J.-L. Retrosynthetic accessibility score (RAscore)–rapid machine learned synthesizability classification from AI driven retrosynthetic planning. *Chem. Sci.* **12**, 3339–3349 (2021).
32. Morris, A. et al. Discovery of sars-cov-2 main protease inhibitors using a synthesis-directed de novo design model. *Chem. Commun.* **57**, 5909–5912 (2021).
33. Krenn, M., Häse, F., Nigam, A., Friederich, P. & Aspuru-Guzik, A. Self-referencing embedded strings (selfies): a 100% robust molecular string representation. *Mach. Learn.* **1**, 045024 (2020).
34. Vaswani, A. et al. Attention is all you need. In *Proc. 31st International Conference on Neural Information Processing Systems* (eds Guyon, I. et al.) 6000–6010 (Curran Associates Inc., 2017).
35. Ying, C. et al. Do transformers really perform badly for graph representation? *Adv. Neural Inf. Process. Syst.* **34**, 28877–28888 (2021).
36. Zhang, L., Xu, D., Arnab, A. & Torr, P. H. Dynamic graph message passing networks. In *Proc. IEEE/CVF Conference on Computer Vision and Pattern Recognition* 3726–3735 (2020).
37. Jacob, P.-M. & Lapkin, A. Statistics of the network of organic chemistry. *React. Chem. Eng.* **3**, 102–118 (2018).
38. Vignac, C. & Frossard, P. *International Conference on Learning Representations* (ICLR, 2022).
39. Chen, S. & Jung, Y. A generalized-template-based graph neural network for accurate organic reactivity prediction. *Nat. Mach. Intell.* **4**, 772–780 (2022).
40. Bickerton, G. R., Paolini, G. V., Besnard, J., Muresan, S. & Hopkins, A. L. Quantifying the chemical beauty of drugs. *Nat. Chem.* **4**, 90–98 (2012).
41. Friesner, R. A. et al. Extra precision glide: docking and scoring incorporating a model of hydrophobic enclosure for protein-ligand complexes. *J. Med. Chem.* **49**, 6177–6196 (2006).
42. Qiang, B. Processed training data for 'Bridging the gap between chemical reaction pretraining and conditional molecule generation with a unified model'. *Zenodo* https://doi.org/10.5281/zenodo.8075067 (2023).
43. Qiang, B. qiangbo1222/Uni-RXN-official V1.0. *Zenodo* https://doi.org/10.5281/zenodo.8113249 (2020).
44. Reymond Group: DRFP. *GitHub* https://github.com/reymond-group/drfp (2023).

Acknowledgements

This work was financially supported by National Key R&D Programme of China (grant no. 2022YFF1203003 (Z.L.) and grant no. 2022YFC2303700 (L.Z.)), Beijing AI Health Cultivation Project (grant no. Z221100003522022 (Z.L.)), Peking University Health Science and StoneWise Technology Joint Laboratory Project (grant no. L202107 (Z.L.)) and the Open Fund of State Key Laboratory of Pharmaceutical Biotechnology, Nanjing University, China (grant no. KF-202304 (Z.L.)).

Author contributions

B.Q. conceived the initial idea for the projects. B.Q. and Y.D. processed the dataset and trained the model. B.H. provided support on computing resources. B.Q. and Y.Z. performed the experiments using the pretrained model and the generative model. Y.Z. analysed the results and B.Q. wrote the manuscript. B.Q., S.S., L.Z. and Z.L. contributed to the revision of the manuscript. The project was supervised by L.Z. and Z.L. All authors participated in discussions.

Competing interests

The authors declare no competing interests.

Additional information

Supplementary information The online version contains supplementary material available at https://doi.org/10.1038/s42256-023-00764-9.

Correspondence and requests for materials should be addressed to Bo Huang or Zhenming Liu.

Peer review information *Nature Machine Intelligence* thanks Esben Jannik Bjerrum and Thomas Blaschke for their contribution to the peer review of this work.